JOURNAL OF Materials CHEMISTRY

A new photo-functional material constituted by a spirooxazine supported on a zirconium diphosphonate fluoride

Pier Luigi Gentili,[a] Umberto Costantino,[b] Morena Nocchetti,[b] Costanza Miliani[a] and Gianna Favaro*[a]

[a]*Laboratorio di Fotofisica e Fotochimica, Dipartimento di Chimica, Università di Perugia, 06123 Perugia, Italy. E-mail: favaro@phch.chm.unipg.it*
[b]*Laboratorio di Chimica Inorganica, Dipartimento di Chimica, Università di Perugia, 06123 Perugia, Italy*

Received 31st May 2002, Accepted 5th July 2002
First published as an Advance Article on the web 9th August 2002

The photochromic behaviour of a spirooxazine (1,3,3-trimethylspiro[indoline-2,3′-[3*H*]naphth[2,1-*b*][1,4]oxazine]) was investigated in a solid matrix at room temperature. The solid matrix belongs to the class of layered zirconium phosphonates and was obtained by slowly decomposing zirconium fluoro complexes in a water–methanol solution containing dissolved $CH_3(CH_2)_7N(CH_2PO_3H_2)_2$ diphosphonic acid. The white powder consists of spherical particles (average diameter 50 μm) made up of lamellar microcrystals of formula $Zr[O_3PCH_2NHCH_2PO_3(CH_2)_7CH_3]F\cdot 0.2H_2O$. The lamellar structure arises from the packing of layers, each constituted by an inorganic bidimensional array with pendant alkyl chains. The spirooxazine, adsorbed onto the solid surface, maintains the thermoreversible photochromic behaviour exhibited in solution (photocolouration under UV irradiation and thermal bleaching in the dark). The microenvironment, generated by the solid phase, influences both the chromaticity and decolouration dynamics of the system. Two absorption bands were observed in the visible: one at about 600 nm, due to the coloured photomerocyanine and the other, shifted to the red (~700 nm), was assigned to J-aggregates of the photomerocyanines, based on temperature effect and spectral position. Both visible absorptions increased under UV irradiation and partially bleached in the dark. The relaxation times, different in the two spectral regions, were longer than in a fluid solution. Biexponential decay kinetics, observed at 610 nm, were explained by assuming that the detachment of the photomerocyanine from the stacks was the rate-determining step of the bleaching reaction for the molecules adsorbed onto the surface of the aggregated lamellae.

Introduction

Photochromic compounds undergo a reversible structural transformation upon absorption of electromagnetic radiation. The reversibility can be thermal, photochemical or both (Scheme 1).

The reversible process A ⇌ B produces significant changes in the chemical–physical properties, the most important being the colour change. Generally, A is a colourless UV light absorbing species, whereas B is coloured and also absorbs visible light. Materials which change colour in response to an external stimulus have been extensively investigated over the last few decades. Incorporating photochromic molecules into solid matrices is a promising way to obtain photo-functionalized chromogenic materials.

The changes that occur in the chemical–physical properties on going from A to B and *vice versa* induce a reciprocal influence on the photochromic behaviour and the characteristics of the microenvironment. The photochromic process is affected by the supramolecular structure of the host matrix, which, in turn, may be affected by the photochromic process with regard to several physical properties.[1] Both photocolouration and thermal bleaching are generally slower when the photochromic molecules are in a solid matrix, compared with their rates in a liquid phase. This effect is more pronounced when the photochromic reaction is accompanied by significant structural changes, especially when the free volume available for the guest is limited, and, if the matrix is a polymer, when the segmental mobility is low.[2] On the other hand, the structural dualism of a photochromic compound affects the surrounding micro-environment, *i.e.* the supramolecular structure of the including matrix.

The aim of this paper was to investigate the properties of a composite system, in which a photochromic compound was incorporated into a layered solid phase, particularly focusing on the effect of the mutual interactions between the two components.

The photochrome investigated, 1,3,3-trimethylspiro[indoline-2,3′-[3*H*]naphth[2,1-*b*][1,4]oxazine], SO, has been extensively studied in solution.[3–7] Its photochromism is based on an electrocyclization reaction (Scheme 2).

The absorption of near UV radiation induces cleavage of the *spiro* C–O bond, yielding a planar photomerocyanine (PM) with a fully delocalized π-electron system, that also absorbs a portion of visible light. A thermal 1,6-electrocyclization restores the initial SO structure. The ring-opening reaction originates from the excited singlet state and leads to PM within

$$A \underset{h\nu_2,\,\Delta}{\overset{h\nu_1}{\rightleftharpoons}} B$$

Scheme 1

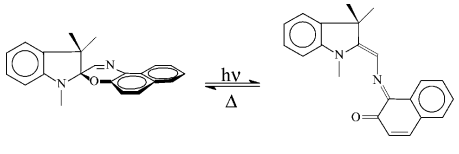

SO PM

Scheme 2

 DOI: 10.1039/b205297k

50 ps after excitation.[8] Theoretical studies have shown that the driving force for the ring-opening reaction is a charge transfer process from the lone pair of the indoline nitrogen to the antibonding orbital of the C2–O bond of the orthogonal oxazine moiety.[9]

Among the various host systems capable of including and/or adsorbing photoactive species, attention has been given to layered compounds that offer two-dimensional expandable interlayer space for organizing the guest species. Much research has been done to intercalate photoactive species onto different layered compounds (smectite clays, hydrotalcite-like compounds, metal phosphates) and the photo-function of the intercalation compounds obtained has been studied.[10] Compared with other layered hosts, zirconium(IV) phosphonates are attractive because they are made-up of a two-dimensional inorganic network that can be functionalized with different organic or metal–organic functions.[11,12] In principle, it is possible to tailor the host to a given guest species by introducing the appropriate functional group. In the present work, a member of a novel family of Zr phosphonates, Zr(IV)-alkyl-amino *N*,*N*-bis(methylene phosphonate) fluoride has been prepared and characterized. This layered compound, made up of hydrophobic monolayers of interdigitated octyl chains, that alternate regularly with the inorganic component, provides the SO guest with a non-polar microenvironment, as well as polar sites in correspondence to the fluoride and phosphonate groups.

Spirooxazines display an unusual fatigue resistance and durability.[13] The characteristics of these compounds make them interesting candidates for use in optical devices such as light filters, image storage systems and computer switches.[14]

Experimental

Materials

The 1,3,3-trimethylspiro[indoline-2,3′-[3*H*]naphth[2,1-*b*][1,4]oxazine] was supplied by Great Lakes Chemical Italia s.r.l. for previous studies[6,7] and was used without further purification.

The solid phase, $Zr[O_3PCH_2NHCH_2PO_3(CH_2)_7CH_3]F\cdot 0.2H_2O$, hereafter referred to as ZrC8, was synthesised using a "soft chemistry" method, under mild processing conditions. The preparation was analogous to that previously applied to synthesise α-zirconium phosphate[15] and phosphonates.[16] The solid octyl-amino-*N*,*N*-bis(methylene phosphonic) acid, prepared according to the procedure described in ref. 17, was dissolved in a mixture of water and methanol (blended in a volume ratio of 1 : 2). A water solution containing fluoro-complexes of zirconium was added. The molar ratios for the synthesis were: P/Zr = 4 and F/Zr = 25. The zirconium concentration was 0.01 mol dm^{-3}. The solution was kept in a closed plastic bottle at 75 °C, for five days. The phosphonate anion replaced the fluoride anions which were removed as HF by light heating. After precipitation, the solid phase was recovered and dried in an oven at 75 °C.

To prepare the SO–ZrC8 composite system, concentrated solutions ([SO] = 9.5×10^{-3} mol dm^{-3}) of the SO in various organic solvents (hexane, ethanol, propanol, and octanol) were equilibrated with the solid phase (average guest/host molar ratio 1 : 2.5) in the dark under magnetic stirring for six days. After this contact period, the solid phase was recovered and air dried.

Apparatus and measurement conditions

X-Ray powder diffraction (XRPD) patterns of wet and dried samples were taken with a computer-controlled Philips PW1710 diffractometer using graphite-monochromated Cu-Kα radiation and operating at 40 kV, 30 mA, step-scan 0.03° 2θ and 1 s counting time.

Surface area and porosity were determined by N_2 adsorption–desorption isotherms at 77 K taken with a Micromeritics ASAP 2010 instrument, after degassing the sample for 1 day at 393 K. Thermogravimeter-differential thermal analysis (TG-DTA) was performed in air using a Stanton Redcroft STA781 instrument at a heating rate of 5 K min^{-1}. CHN elemental analyses were carried out with a Carlo Erba Model 1106 Analyser.

The absorption spectra were recorded using a Perkin-Elmer Lambda 16 spectrophotometer, equipped with a Perkin-Elmer accessory for reflectance measurements. The irradiation was carried out with a high pressure mercury lamp, filtered by a large-band filter transmitting in the 230–400 nm wavelength range. The powdery sample was packed in a spectrophotometric cell (0.1 cm path length). The kinetics of the thermal ring-closure reaction were recorded spectrophotometrically following the colour bleaching of the irradiated sample at a fixed wavelength immediately after removing the irradiating source.

Scanning electron microscopy (SEM-EDS) investigations were performed on a Philips XL30 scanning electronic microscope fitted with a LaB_6 electron gun. The powder samples were attached directly to the stub using a conductive carbon glue (Carbon Cement Leit-C, Neubauer Chemikalien).

Results and discussion

Structural characteristics of the ZrC8 matrix

Octyl-amino-*N*,*N*-bis(methylene phosphonic) acid, $C_8H_{17}N(CH_2PO_3H_2)_2$, is an amphiphilic molecule composed of polar PO_3H_2 heads and a hydrophobic alkyl chain. In the solid state, the molecules auto-assemble in a layered structure as evinced by the analysis of the XRPD pattern shown in Fig. 1a. Recently obtained structural data[18] for the homologous compound

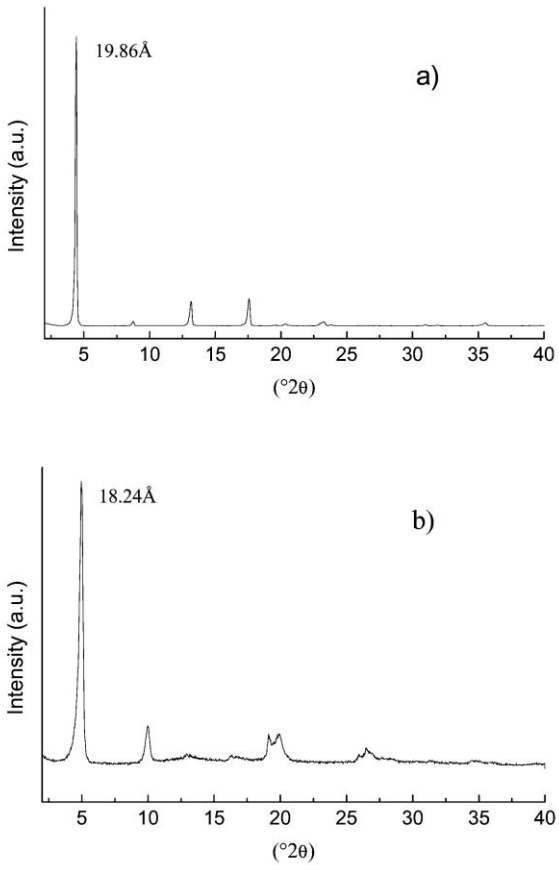

Fig. 1 X-Ray powder diffraction patterns of $C_8H_{17}N(CH_2PO_3H_2)_2$ (a) and ZrC8 (b).

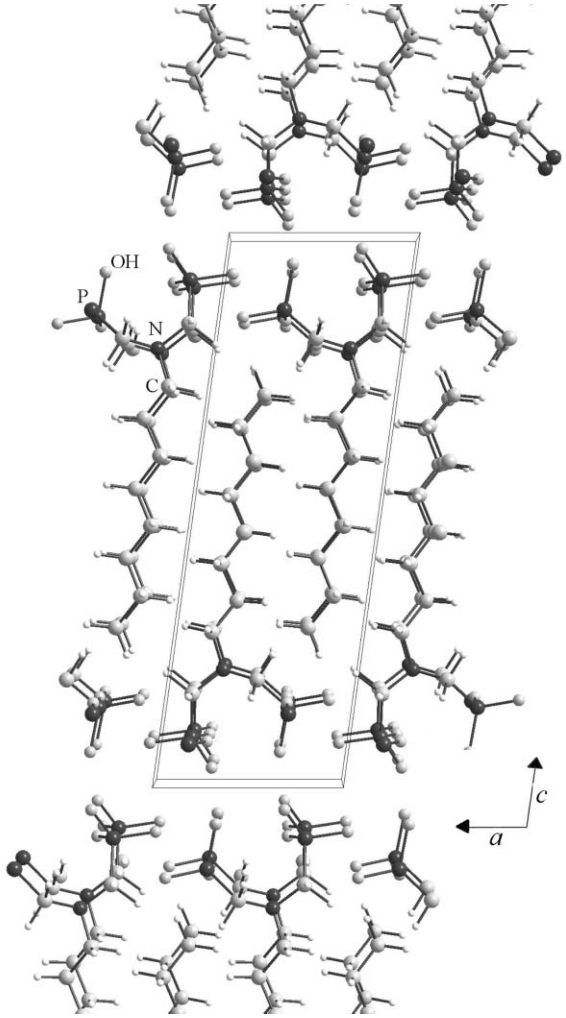

Fig. 2 Computer-generated model of $C_8H_{17}N(CH_2PO_3H_2)_2$ showing the interdigitated alkyl chain, and the phosphonate polar heads. The unit cell is highlighted.

$C_5H_{11}N(CH_2PO_3H_2)_2$, allow one to presume that the octylamine derivative has a similar layered structure, in which each layer is made up of a mono-film of interdigitated alkyl chains with the polar head situated on both sides of the monofilm, as shown in Fig. 2.

Precipitation of the diphosphonic acid with zirconium salt (see Experimental) causes the Zr(IV) to be inserted between the polar heads of the opposite lamellae of the solid acid, forming Zr–O–P bonds. The monofilm of interdigitated octyl chains remains practically unchanged. The X-ray powder diffraction spectrum of ZrC8 (see Fig. 1b) shows that the solid still has a layered structure with an interlayer distance of 18 Å, which is shorter than that of the precursor acid (20.6 Å). When Zr is introduced between the polar heads, the phosphorus–phosphorus distance between adjacent lamellae is reduced, due to formation of covalent bonds.

Elemental and thermogravimetric analysis gave the formula $Zr[O_3PCH_2NHCH_2PO_3(CH_2)_7CH_3]F{\cdot}0.2H_2O$. A structural model was derived by taking into account data from the homologous $Zr[O_3PCH_2NHCH_2PO_3(CH_2)_4CH_3]F$ compound whose crystal structure will be published elsewhere.[19] According to the model, each layer is made up of Zr atoms and each Zr octahedrally coordinates six atoms: five oxygen atoms, belonging to five different phosphonates, and a fluorine atom. Every two phosphonate groups, belonging to the diphosphonic acid, use five oxygen atoms to link five zirconium atoms and one oxygen atom to link a hydrogen atom that protonates the nitrogen of the adjacent amino group. The alkyl chains are pendant from both sides of the inorganic portion of the layer

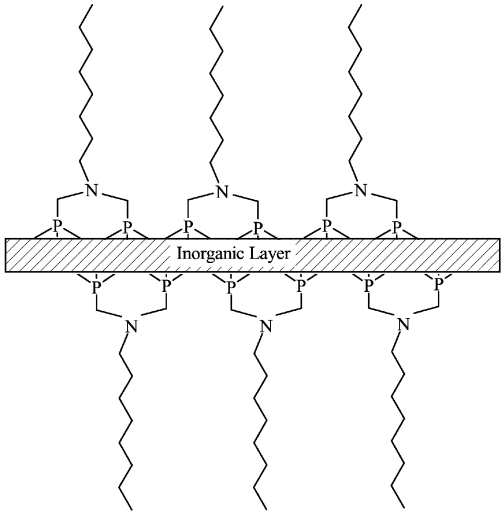

Fig. 3 Schematic model of the ZrC8 sheet structure.

(see Fig. 3). The layers are packed in such a way that the alkyl chains of one lamella interpenetrate those of the adjacent lamellae.

The morphology of the ZrC8 particles obtained from the synthesis was observed by scanning electron microscopy (Figs. 4a and 4b). The particles are approximately spherical

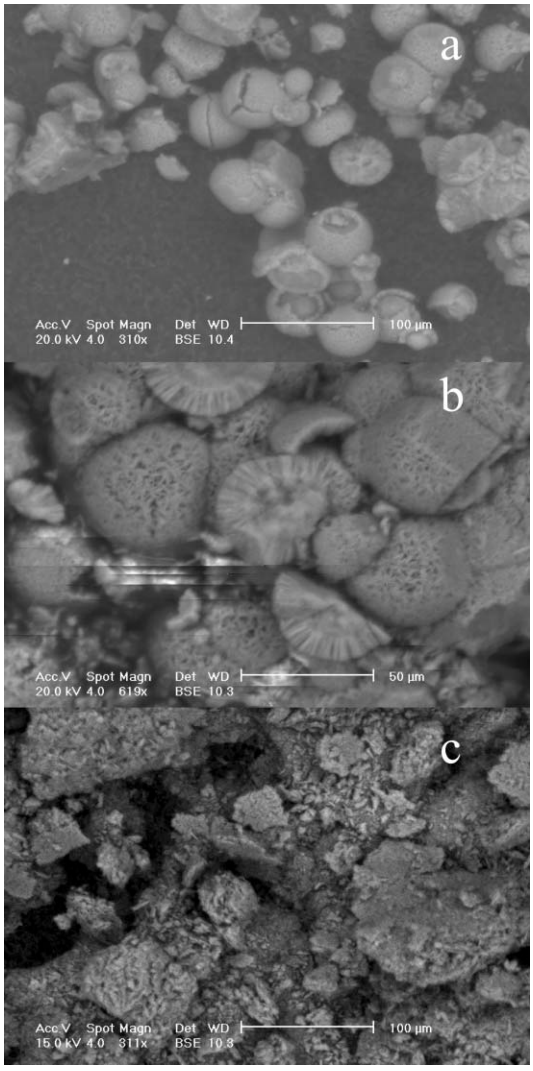

Fig. 4 SEM back-scattered electron images showing the microcrystal structure of ZrC8. Globular structures: (a) 310× and (b) 619×. After cracking, (c) 311×.

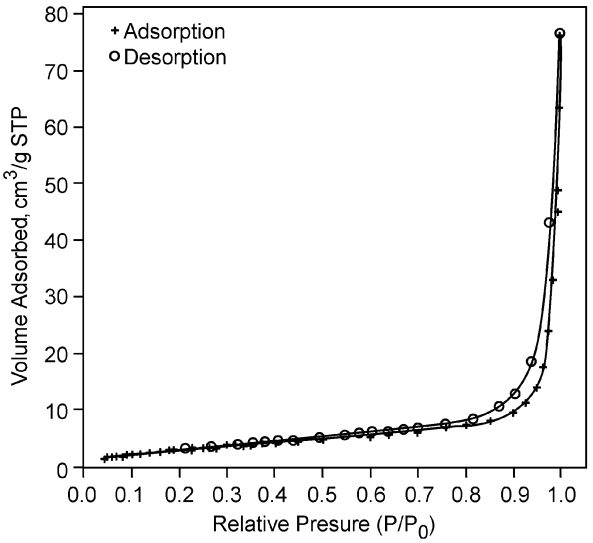

Fig. 5 Adsorption and desorption of nitrogen on ZrC8 at 77 K.

with an average diameter of 50 μm. Each particle (globule) consists of a central homogeneous core surrounded by an outer, more ordered shell of aggregated sheets. The core and the shell seem to have the same chemical composition, as shown by X-ray fluorescence. The globule, as a whole, resembles a micelle, where surfactant molecules are assembled in an approximately spherical shape, with the polar head groups on the surface and the aliphatic tails extending towards the core. In the present case, the sheet takes on the role of a surfactant molecule. The edges of the aggregates have a partial polar character due to the phosphonate and fluoride groups linked to Zr atoms. The lamellar microcrystals, growing in a polar environment (a water–methanol mixture), tend to associate through the less polar surfaces, leaving the more polar superficial portion facing outwards, towards the solution. The more ordered external part of the microcrystals is probably due to a slower growth rate. Once the globules were broken by grinding them in an agate mortar, the lamellar structure became more evident (Fig. 4c). The specific surface area and porosity of the ZrC8 microcrystals were determined through the nitrogen adsorption–desorption isotherms at 77 K (see Fig. 5). The BET treatment[20] of the isotherms gave a specific surface area of $12.74 \pm 0.09\ m^2\ g^{-1}$. The *t*-plot analysis,[20] performed by using α-zirconium phosphate as reference material,[21] provided a negligible micropore volume, in agreement with the low amount of nitrogen adsorbed at low pressure. The narrow hysteresis observed in the adsorption–desorption isotherms (see Fig. 5) indicated that the solid phase has a negligible mesoporosity. Accordingly, BJH analysis[21] gave a very low mesopore volume and the few mesopores observed had dimensions in the 20–50 Å. range. The microcrystals had macropores that were also visible in the electron microphotographs (see Fig. 4).

Structural characteristics of the SO–ZrC8 composite material

When the photochrome-containing solution is in contact with the ZrC8 solid phase, the distribution equilibrium of the solute between the two phases is established. A solid layered host can incorporate the guest species into the interlayer region (intercalation) and/or onto the surface (adsorption). Several attempts have been made to intercalate the photochrome by changing the solvent and equilibration times. In order to facilitate the insertion of SO molecules into the interlayer region, solvents such as propanol and octanol, able to swell ZrC8 (the interlayer distance increases from 18 to 23.7 and 27.6 Å, respectively), were also used. However, all the dried solid phases, obtained by ZrC8 contact with the SO solutions, exhibited an interlayer distance of about 18 Å, that is, the characteristic value of pure ZrC8. This indicates that SO molecules were not intercalated into the host solid matrix.

Lack of intercalation may be the result of steric constrictions and/or microenvironment polar interactions. In some cases, for similar molecules, intercalation in the interlayers of Montmorillonite and MgAl layered double hydroxide was achieved due to the presence of ionogenic functional groups.[22–24]

The amount of SO adsorbed per mole of the ZrC8 host was calculated to be 0.03–0.05 moles by using thermogravimetric and UV-VIS spectrophotometric analyses (carried out on the liquid phase before and after the contact with the solid phase). The area covered by the adsorbed SO was calculated by considering that one mole of host has an external surface area of $12.74\ m^2\ g^{-1} \times 424\ g\ mol^{-1} = 5.4 \times 10^3\ m^2\ mol^{-1}$, while the SO is approximately described as a three-dimensional molecule (13.93 Å × 7.12 Å × 6.4 Å, from the molecular structure optimized with the Hyperchem program). Since efficient interactions between host and guest stabilize the supramolecular structure, the adsorbtion should use the most guest surface possible. Therefore, every SO molecule should cover an average area of 14 Å × 7 Å = 98 $Å^2$, that is, about $10^{-18}\ m^2$. Based on these values, one mole of ZrC8 would be completely covered by 0.009 moles of SO. The experimental value of SO moles adsorbed onto ZrC8 (0.03–0.05 moles) exceeds the predicted saturation value (0.009) which suggests that photochrome aggregates can be formed on the ZrC8 host surface.

Spectral and photochromic behaviour of the SO–ZrC8 composite

In diluted SO organic solutions ($\sim 10^{-5}$ mol dm^{-3}), at room temperature, only the spectrum of the colourless form is detectable. In concentrated solutions ($\sim 10^{-3}$ mol dm^{-3}), the band of the coloured PM is observed and it increases with increasing temperature. Its appearance is due to establishing the thermal equilibrium between the open and closed forms. The equilibrium constant is greater in a polar solvent than in a non-polar one ($K \approx 10^{-4}$ in ethanol and $K \approx 10^{-5}$ in toluene, at 298 K), due to solvent stabilization of the dipolar transition state.[6] Under UV irradiation, the production of the photomerocyanine is detectable by spectrophotometry, even in diluted solutions. The maximum PM absorption wavelength, observed at 613 nm in a polar and protic solvent, EtOH, shifts to the blue (585 nm) in a non-polar solvent, methylcyclohexane[7] (see Table 1). That is, this molecule exhibits marked positive solvatochromism. When the irradiation is discontinued, the rate of colour bleaching is on the order of $2 \times 10^{-1}\ s^{-1}$ at room temperature.[6]

The reflectance UV-VIS spectra of the powdery samples showed the characteristic absorption of SO in the UV region with, more or less pronounced, but significant, absorptions at longer wavelengths. Two bands were observed in the visible region, one at 610 nm and the other (two-peaked) around 700 nm and their relative contribution to the overall absorption depended on the sample. The different patterns that were obtained could have been due to the solvent used, the molar ratio between the photochrome and ZrC8, the concentration of the photochrome solution and the duration and temperature of

Table 1 Spectral (λ_{max}) and kinetic (k_Δ) properties of the PM in various media at 293 K

Medium	λ_{max}/nm	k_Δ/s^{-1}
ZrC8	610	$0.0015(k_{(PM)_n})/(0.014k_{(PM)})$
Ethanol[a]	613	0.041
Methylcyclohexane[a]	585	0.052
AOT (microemulsion)[b]	600	0.16
Gel[c]	613	0.15

[a]Taken from ref. 7. [b]Taken from ref. 31. [c]Taken from ref. 32.

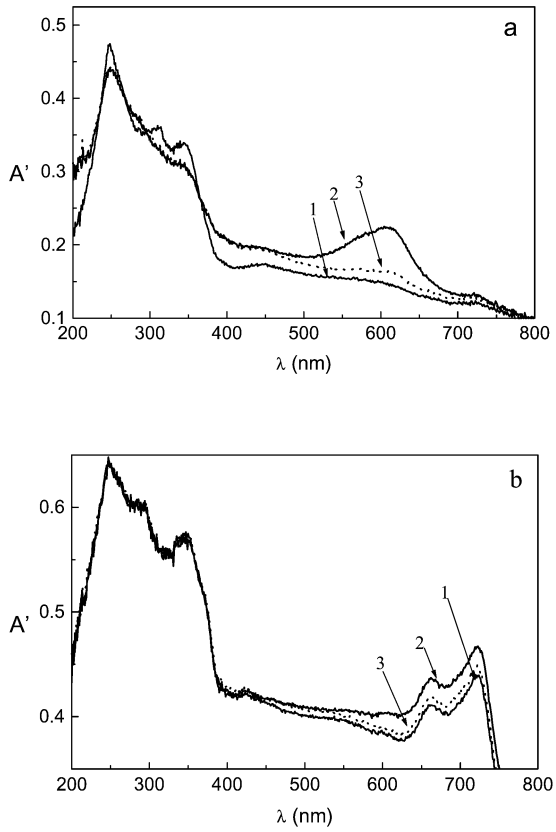

Fig. 6 Reflectance spectra ($A' = \log 1/R$, R is the reflectance signal) of the SO–ZrC8 composite obtained from propanol (a) and from hexane (b). (1) before irradiation; (2) immediately after 15 min irradiation; (3) after 15 min in the dark.

the contact period between the liquid and solid phases. Examples of different spectral patterns exhibited by composites obtained from propanol and hexane solutions, respectively, are shown in Fig. 6. By irradiating the powders, the formation (or increased intensity) of the colour bands was observed. When the irradiation was discontinued and the samples kept in the dark, the colour bands bleached slowly, but did not completely disappear. A residual absorption persisted for an indefinite time.

The band at 610 nm is attributed to the coloured PM form. Its position is close to that found in polar solvents (Table 1) and this points to a polar nature of the adsorption sites. The appearance of the PM absorption, even without irradiation, is due to the relatively high SO concentration used to synthesise the composite (the contact solutions were coloured). The bands located at higher wavelengths are attributed to aggregates of the PM. It is well known that merocyanines tend to associate forming molecular aggregates with a stack-like structure.[25] If the molecular dipoles are aligned in parallel, the aggregate absorption is red-shifted compared to that of the isolated PM (J-aggregates). In the case of anti-parallel dipole interactions, the absorption shifts to the blue (H-aggregates). In accordance with the observed red-shift, the assemblies which were present in the composite material are assigned to J-type aggregates of the photomerocyanine form, $(PM)_n$. Since the aggregate bands were not observed in the solutions kept in contact with the solid phase, it can be inferred that aggregation is induced by adsorption: weak host–guest interactions favour guest–guest interactions. Both J- and H-aggregates of PMs were detected for some spiropyrans embedded in bilayer-clay matrices,[26] as well as in other solid matrices.[27] Since the formation of aggregates in organized host media may affect the energy and relaxation paths of the lowest excited states, the chromatic properties and colourability of a guest photochromic molecule may change.

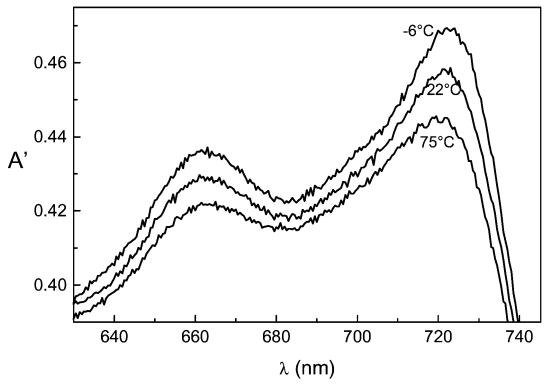

Fig. 7 Temperature effect on the aggregate absorption of a SO–ZrC8 powdery sample obtained through contact of ZrC8 with a concentrated SO hexane solution.

Further support for attributing the red-shifted absorptions to aggregates comes from the study of temperature effects. Cyclic temperature variations produce reversible variations of stack absorption. As shown in Fig. 7, temperature increase induces a partial dissociation of the aggregates as expected for such an endothermal process.

The thermal bleaching kinetics was followed at both the monomer ($\lambda = 610$ nm) and aggregate ($\lambda = 722$ nm) absorption maximum wavelengths. At 722 nm, mono-exponential decay, $k_{(PM)_n} = 0.0015 \pm 0.0003\ s^{-1}$ at 21 ± 1 °C, was observed for all samples. At 610 nm, the wavelength characteristic of the PM monomer, deviations from first order kinetics were observed. The bleaching process could be better described by a bi-exponential function. The two exponential coefficient values, $0.0016 \pm 0.0003\ s^{-1}$ and $0.014 \pm 0.003\ s^{-1}$, were obtained from a non-linear fit computerized program and are the average of the values determined for different samples at 21 °C. Examples of bleaching kinetics at the two wavelengths are shown in Fig. 8.

The fading of the aggregate band (722 nm) is attributed to

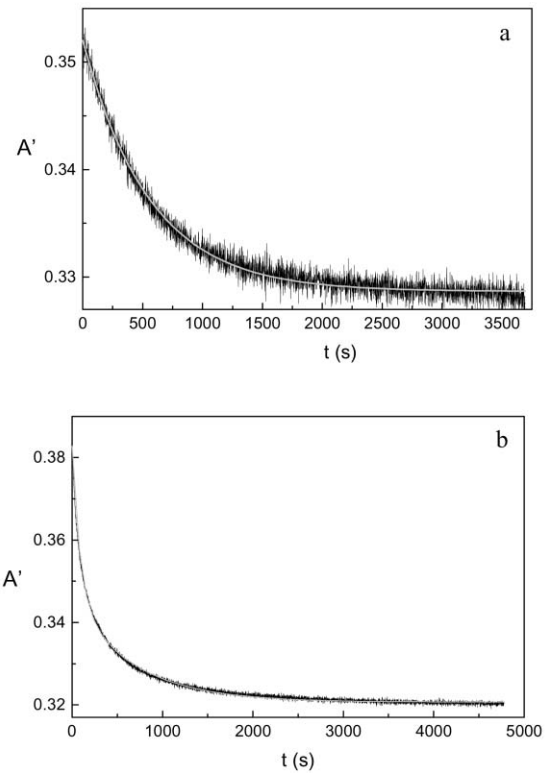

Fig. 8 Kinetics of thermal bleaching of the coloured forms of the photochrome adsorbed on ZrC8 followed at 722 nm (a) and 610 nm (b).

the PM molecules detaching from the stacks:

$$(PM)_n \rightarrow (PM)_{n-1} + PM$$
$$k_{(PM)_n} = (0.0015 \pm 0.00030)\ s^{-1}$$

The bleaching observed at 610 nm is due to the closure of the PMs, formed from the SOs by irradiation, or detached from the $(PM)_n$ stacks:

$$PM \rightarrow SO\ k_{PM} = (0.014 \pm 0.003)\ s^{-1}$$

The slowest detachment process is the rate-determining step of the bleaching kinetics for the PMs originating from the aggregate. This can be reasonably inferred based on the similarity of $k_{(PM)_n}$ and the slow decay component at 610 nm. The rate equations at 722 nm are given by eqn. (1) and at 610 nm by eqn. (2):

$$-d[(PM)_n]/dt = k_{(PM)_n}[(PM)_n] \quad (1)$$

$$-d[PM]/dt = k_{PM}[PM] - k_{(PM)_n}[(PM)_n] \quad (2)$$

Integration of eqn. (1) yields eqn. (3).

$$[(PM)_n]_t = [(PM)_n]_0 e^{-k_{(PM)_n}t} \quad (3)$$

Insertion of (3) into eqn. (2) and integration leads to a bi-exponential function, eqn. (4), in agreement with the experimental findings.

$$[PM]_t = \{[PM]_0 - k_{PM}[(PM)_n]_0/(k_{PM} - k_{(PM)_n})\}e^{-k_{PM}t} + \{k_{PM}[(PM)_n]_0/(k_{PM} - k_{(PM)_n})\}e^{-k_{(PM)_n}t} \quad (4)$$

Biexponential bleaching processes have frequently been found in photochromic systems embedded in solid matrices. Two-component kinetics can be explained in terms of two (or more) kinds of microscopic environments, with different micro-polarity and micro-viscosity, where the relaxing species encounter different energy barriers to closure.[28,29] In a polymer matrix, the experimental multiple/double exponential decay was explained by Krongauz *et al.*[27] assuming that decolouration occurred by the successive detachment of PM molecules from H-aggregates at a rate which decreased with increasing chain length. An interpretation, similar to that of the present work, was proposed to explain the dynamic behaviour of a nitrospiropyran in a concentrated solution of a non-polar solvent.[30] In that case, however, the detachment of PM from the aggregate was faster than the PM closure.

The reversible behaviour of this material to light and temperature stimulations suggests that both the closed and open forms are adsorbed and even aggregated onto the solid surface. Due to the hydrophobic nature of the organic chains, van der Waals interactions are responsible for the adsorption of the closed form, while dipolar interactions, with the emerging phosphonate and fluoride groups linked to the Zr atoms, also contribute to the adsorption of the more polar, plate-like merocyanine structures.

The monomer relaxation constant in ZrC8 is compared with those obtained in different media, such as polar and non-polar solvents,[7] micelles,[31] and a gel,[32] in Table 1. The table shows that the slowest k_Δ values are those reported for the material investigated in this work. For a molecule, such as this that has a quinoid ground state, the transition state is more stabilized in polar sites where the activation energy decreases, thus the rate increases. On the other hand, high viscosity and space-constrictions may retard the closure process. The data in Table 1 show that the second factor is the most important in the solid matrix since, while the absorption is red-shifted as in a polar medium, the closure rate is slow. The opposite behaviour was observed in a gel, where the polarity effect dominated the viscosity effect and the decay was very fast.

Conclusions

In this work a newly synthesised layered solid phase was photofunctionalized by inclusion of a photochromic compound. The microenvironment, into which the compound was included, assumed the typical photosensitivity of the photochrome, while the photochromic behaviour was influenced by the surrounding host matrix through mutual supramolecular interactions.

The spirooxazine adsorbed onto the sheet-structured solid phase of ZrC8 maintained the reversible photochromic behaviour, but the chromatic properties changed due to the formation of J-aggregates which absorbed at longer wavelengths. The dynamic properties also changed due to the constraints in the solid matrix. The lifetime of the metastable coloured PM increased. The J-aggregation onto the ZrC8 surface also contributed to slowing down the relaxation of PM because the rate-determining step for the successive closure of the open form was the slow detachment of the PM from the stacks.

Finally, the organic–inorganic composite systems prepared in this work could have potential applications, since the solid phase can be easily handled and exhibits photochromism even after several months. The colourability of such material could be improved by using suitably substituted spirooxazines.

Acknowledgements

This research was funded by the Ministero per l'Università e la Ricerca Scientifica e Tecnologica (Rome) and the University of Perugia in the framework of the Programmi di Ricerca di Interesse Nazionale (project: Mechanisms of Photoinduced Processes in Complex Matrices) and by the Italian National Research Council.

References

1 K. Ichimura, in *Photochromism. Molecules and Systems*, eds. H. Dürr and H. Bouas-Laurent, Elsevier, Amsterdam, 1990, p. 903.
2 C. Eisenbach, *Ber. Bunsen. Phys. Chem.*, 1980, **84**, 680–690.
3 N. Y. C. Chu, *Can. J. Chem.*, 1983, **61**, 300–305.
4 A. Kellmann, F. Tfibel, R. Dubest, P. Levoir, J. Aubard, E. Pottier and R. Guglielmetti, *J. Photochem. Photobiol., A: Chem.*, 1989, **49**, 63–73.
5 F. Wilkinson, J. Hobley and M. Naftaly, *J. Chem. Soc., Faraday Trans.*, 1992, **88**, 1511–1517.
6 G. Favaro, F. Masetti, U. Mazzucato, G. Ottavi, P. Allegrini and V. Malatesta, *J. Chem. Soc., Faraday Trans.*, 1994, **90**, 333–338.
7 G. Favaro, V. Malatesta, U. Mazzucato, G. Ottavi and A. Romani, *J. Photochem. Photobiol., A: Chem.*, 1995, **87**, 235–241.
8 S. Aramaki and G. H. Atkinson, *Chem. Phys. Lett.*, 1990, **70**, 181–186.
9 V. Malatesta, G. Ranghino, U. Romano and P. Allegrini, *Int. J. Quantum Chem.*, 1992, **42**, 879–887.
10 M. Ogawa and K. Kuroda, *Chem. Rev.*, 1995, **95**, 399–438.
11 G. Alberti, in *Solid-state Supramolecular Chemistry: Two- and Three-dimensional Inorganic Networks*, vol. 7, eds. G. Alberti and T. Bein of the series *Comprehensive Supramolecular Chemistry* (chairman ed. J.-M. Lehn), ch. 5, Pergamon, Elsevier Science Ltd., 1996, pp. 151–187.
12 A. Clearfield, *Prog. Inorg. Chem.*, 1998, **47**, 371–510.
13 N. Y. C. Chu, in *Photochromism. Molecules and Systems*, eds. H. Dürr and H. Bouas-Laurent, Elsevier, Amsterdam, 1990, p 493.
14 R. Guglielmetti, in *Photochromism. Molecules and Systems*, eds. H. Dürr, and H. Bouas-Laurent, ed. Elsevier, Amsterdam, 1990, p. 855.
15 G. Alberti and E. Torracca, *J. Inorg. Nucl. Chem.*, 1968, **30**, 317–319.
16 G. Alberti, S. Allulli, U. Costantino and N. Tomassini, *J. Inorg. Nucl. Chem.*, 1978, **40**, 1113–1117.
17 K. Moedritzer and A. Irani, *J. Org. Chem.*, 1966, **311**, 1603–1607.

18 U. Costantino, R. Renghi and R. Vivani, to be published. A preliminary account is in *Proceedings of GFECI 2001*, Balaruc les Bains, Societè Francaise de Chemie, 2001, p. 56.
19 U. Costantino, M. Nocchetti and R. Vivani, *J. Am Chem. Soc.*, 2002, **124**, 8428–8434.
20 S. J. Gregg and K. S. W. Sing, *Adsorption, Surface area and porosity*, Academic Press, New York, 2nd edn., 1982.
21 F. Marmottini, in *Multifunctional Mesoporous Inorganic Solids*, eds. C. A. C. Sequeira and M. J. Hudson, Kluwer Academic Publishers, Netherlands, 1993, pp. 37–48.
22 K. Takagi, T. Kurematsu and Y. Sawaki, *J. Chem. Soc., Perkin Trans. 2*, 1991, 1517–1522.
23 H. Tagaya, T. Kuwahara, S. Sato, J. Kadokawa, K. Masa and K. Chiba, *J. Mater. Chem.*, 1993, **3**, 1317–318; H. Tagaya, S. Sato, T. Kuwahara, J. Kadokawa, K. Masa and K. Chiba, *J. Mater. Chem.*, 1994, **4**, 1907–1911.
24 H. Nishikiori, R. Sasai, N. Arai and K. Takagi, *Chem. Lett.*, 2000, 1142–1143.
25 D. M. Sturmer and D. W. Heseltine, in *The Theory of the Photographic Process*, ed. T. H. James, Macmillan, New York, 1977, pp. 194–234.
26 H. Tomioka and T. Itoh, *J. Chem. Soc., Chem. Commun.*, 1991, 532–533.
27 H. Eckhardt, A. Bose and V. A. Krongauz, *Polymer*, 1987, **28**, 1959–1964.
28 A. Plonka, *Chem. Phys. Lett.*, 1988, **151**, 466–468.
29 M. Levitus and P. F. Aramendia, *J. Phys. Chem. B*, 1999, **103**, 1864–1870.
30 H. Sato, H. Shinohara, M. Kobayashi and T. Kiyokawa, *Chem. Lett.*, 1991, 1205–1208.
31 G. Favaro, F. Ortica and V. Malatesta, *J. Chem. Soc., Faraday Trans.*, 1995, **91**, 4099–4103.
32 F. Ortica and G. Favaro, *J. Phys. Chem. B*, 2000, **104**, 12179–12183.